ACS APPLIED MATERIALS & INTERFACES

Letter

www.acsami.org

Characterization of Ion Profiles in Light-Emitting Electrochemical Cells by Secondary Ion Mass Spectrometry

Samuel B. Toshner,[†] Zihua Zhu,[‡] Ilya V. Kosilkin,[§] and Janelle M. Leger*[,†]

[†]Department of Physics and Astronomy, Western Washington University, Bellingham, Washington 98225-9164, United States

[‡]Environmental Molecular Sciences Laboratory, Pacific Northwest National Laboratory, 3335 Q Avenue, Richland, Washington 99354, United States

[§]Department of Chemistry, University of Washington, Box 351700, Seattle, Washington 98195-1700, United States

ABSTRACT: Ion profiles in polymer light-emitting electrochemical cells are known to significantly affect performance and stability, but are not easily measured. Here, secondary ion mass spectrometry is used to investigate ion profiles in both dynamic and chemically fixed junction devices. Results indicate lower reversibility of dynamic junctions and a more significant time delay for ion redistribution than previously expected, but confirm the complete immobilization of ions in chemically fixed junction devices. When compared with prior studies analyzing the electric field profiles in similar devices, these results help to elucidate the roles of ion distribution and electrochemical doping in LECs.

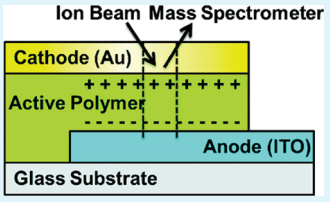

KEYWORDS: *polymer light-emitting electrochemical cell (LEC), organic electronics, electrochemical doping, conjugated polymers, secondary ion beam mass spectrometry*

Semiconducting polymers are known to offer advantages over conventional inorganic semiconductors, as they are solution processable and are therefore compatible with more cost-effective manufacturing processes.[1−3] Another advantage is the ability to conduct ions, an important property for a class of emerging technologies known as 'iontronic' applications.[4,5] Light-emitting electrochemical cells (LECs) are one example of a device in which the active semiconducting polymer is blended with an ionic material.[6] When a voltage is applied, the ions diffuse through the polymer layer and accumulate at the electrode interfaces. This has the effect of reducing charge injection barriers, either via electrochemical doping (with the dissociated salts serving as counterions), or by the establishment of a dipole field induced by the presence of uncompensated ions concentrated at the electrode interfaces.[6−9]

In traditional polymer LEC systems, inorganic salts such as lithium trifluoromethanesulfonate (triflate) are often used. The ions generated from the dissociation of the salt in such systems remain mobile provided that the device is operated at or above the glass transition temperature of the supporting electrolyte, resulting in ion profiles that are dynamic. Specifically, ions accumulate with higher density at the electrodes when higher voltages are applied; similarly if the voltage is removed or reversed, the ion profile will relax or reestablish at the opposite electrodes, respectively. It is well-established that the ion profiles in electrochemical devices are an important factor in determining ultimate device performance and stability. For example, high applied voltages in these mobile systems lead to large ion concentrations at the electrodes and potentially increased degradation due to overdoping and electrochemical side reactions, particularly for ionic liquid based systems.[10−18] In addition, the dynamic nature of the ion profile leads to emission zones that shift with the magnitude of the applied voltage, leading to challenges realizing effective and well-controlled multilayer systems.[19−21]

In addition to the potential instability and limited control associated with dynamic junctions, the relaxation of established ion profiles with removal of external bias in these LECs leads to impractically long turn-on times and disallows the use of these systems in photovoltaic applications. Therefore, fixed junction LECs, or LECs in which the ions are immobilized following the establishment of an appropriate distribution, have been explored.[5,22−29] Several strategies for achieving a fixed junction have been presented in the literature. Recently, we demonstrated the synthesis of a novel polymerizable ionic liquid (PIL) for application to fixed junction LECs.[27] PILs are organic salts with a polymerizable moiety that have a melting point below 100 °C, and belong to a class of ion-paired monomers (IPMs) that have been demonstrated as promising candidates for chemically fixed junction LECs.[28,29] It is believed that a covalent bond is formed in situ between the IPM and the polymer during the initial electrochemical doping event, immobilizing the counterions and thereby creating a chemically fixed junction.[28−30] Current−voltage curves are the primary evidence that ion distributions remain stable in fixed junction devices, as they are typically rectified for fixed junction devices but symmetric for dynamic junctions. Scanning kelvin probe microscopy (SKPM) studies have also shown that for dynamic Li triflate devices, potential profiles return to equilibrium very quickly following electrode grounding, whereas fixed-junction IPM devices maintain their potential profiles.[30−32] Although

Received: October 24, 2011
Accepted: February 28, 2012
Published: March 2, 2012

the formation of truly fixed junctions in IPM-based devices have therefore been confirmed, the correlation between electrical properties and ion profiles has not been fully established. Further, to what extent the established ion distribution in a working device depends on the charging voltage is not known.

Understanding ion profiles in LECs is clearly important for further development of the technology, including not only traditional conjugated polymer-based dynamic and fixed junction systems, but also systems such as transition metal based small molecule ionic devices and ion-functionalized conjugated polymer or polyelectrolyte based systems in which the factors governing ionic motion may be fundamentally different from the systems studied here.[24,33−39] While a general correlation between ion profiles and device performance in LECs is well established, currently little is known directly about how ions move and precisely how they accumulate in working devices. However, because direct profiling of ion distributions in organic films is very difficult, previous studies have relied on indirect evidence of the spatial distribution of ions within the polymer, such as evidence of electrochemical doping or profiles of the electric field. Although these measurements will indicate the presence or absence of unpaired counterions, they will not provide information about counterion concentration, nor the possible presence of nondissociated ions, though these factors are important for device performance. Here we are able to directly measure the spatial profiles of ions in LECs measured after ion relaxation using time-of-flight secondary ion mass spectrometry (ToF-SIMS). In SIMS, by sputtering the sample with a focused ion beam and monitoring the secondary ions, a depth profile of system components can be obtained. SIMS has already been established as a successful method for characterizing organic devices, specifically interface composition, layer and phase mixing, and decompostition.[40−42] In this work, we study ion profiles for LECs using both Li triflate and the PIL allyltrioctylammonium allylsulfonate (ATOA-AS) in order to understand the reversibility and voltage-dependent ion distributions in these systems.

LECs were made in the traditional vertical sandwich-style configuration so that SIMS would provide a mapping along the ion profiles within the device (Figure 1a). Two types of materials systems were studied, a blue-emitting spiro triphenyldiamine (TPD) copolymer with a lithium triflate/trimethylolpropane ethoxylate (TMPE) electrolyte, and a green-emitting polyphenylenevinylene (PPV)/ polyfluorene (PF) copolymer with an ATOA-AS electrolyte.[10] Voltages of 5−15 V were applied to devices under inert atmosphere, with the ITO serving as anode when positively biased, for 1−3 min. This voltage application initiates the ion migration and electrochemical doping and is referred to as "charging" the device. After device charging, the SIMS measurement is performed a minimum of 2 h after charging, limited by the experimental setup procedure. Sputtering was performed through the active area of each pixel, beginning at the gold electrode and continuing through the polymer layer to the ITO electrode. For positive ion depth profiling, electrodes were identified as regions containing high counts of Au^+ or $^{113}In^+$ ions, whereas the polymer layer was distinguished by C^+, H^+, and Li^+ ions (Figure 1b). For negative ion depth profiling, electrodes were detected with Au^- and SnO_2^- ions, and the polymer layer by C^-, H^-, and the cation marker CN^- (Figure 1c). In this way, the spatial boundaries of the polymer layer could be determined, and a fractional depth was calculated to

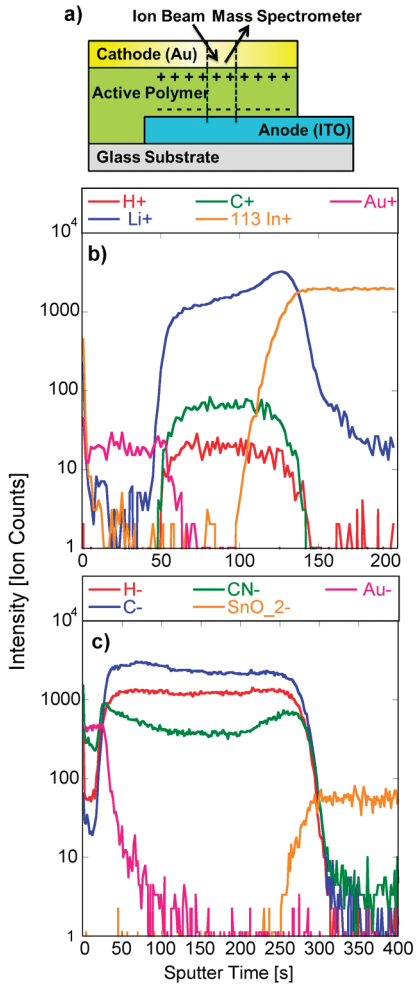

Figure 1. (a) Device schematic including sputtered section of the active area, and ion counts as a function of time (indicating depth) for (b) positive and (c) negative ions. Both scans were carried out on uncharged devices.

normalize the *x*-axis for comparison across different device measurements. Because the cation of lithium triflate is the only lithium-containing compound in the dynamic junction LEC and the cation of ATOA-AS in the only nitrogen-containing compound in the fixed junction LEC, Li^+, and CN^- were used as unique identifiers for the cations in our dynamic and fixed junction LECs, respectively. Anion detection was attempted for both electrolyte systems through the mapping of S^-; however, the signal-to-noise for this measurement was too low to draw reliable conclusions. Future experiments will include attempting to measure alternative anion markers for these systems.

Interestingly, for Li^+ devices, the intrinsic profile shows higher concentrations of the cation on the ITO side of the device prior to charging, which could be the result of the salt accumulating toward the substrate during spin-casting. However, given that this apparent buildup appears to a lesser extent in other scans as well, it may instead be caused by changes in the detection rate that take place at the interface with the ITO electrode. Although this issue currently inhibits our ability to quantitatively analyze ion profiles as a function of depth in the device, we found the measured profiles to be highly reproducible. Therefore, we restrict our attention to sample-to-sample changes in peak intensity for the purposes of this study. Li^+ profiles for pixels charged under forward bias

dx.doi.org/10.1021/am201469t | ACS Appl. Mater. Interfaces 2012, 4, 1149−1153

reveals a systematic buildup with increasing voltage along the cathode (Au) that persists for at least two hours after charging (Figure 2a). The narrow profile along the electrode is in good

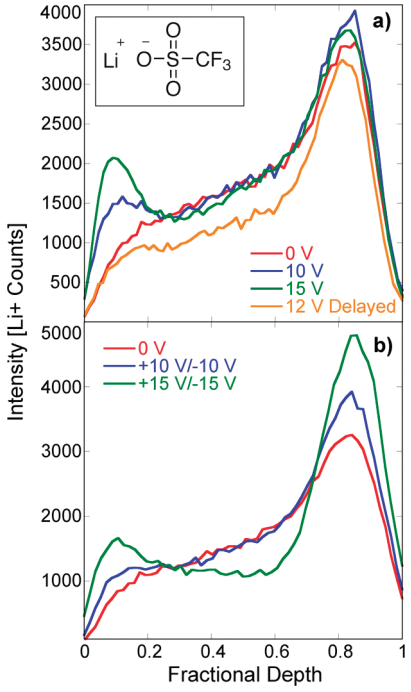

Figure 2. Relative intensities of the Li^+ cation as a function of fractional depth into the polymer layer of Li triflate LECs as a function of charging voltage, (a) for devices charged under using a forward bias and (b) for devices charged first under forward bias followed by charging under reverse bias. Scans taken approximately 2–3 h after charging except where noted. Inset shows molecular structure of Li triflate.

agreement with previous studies.[21,30] However, the measurable retension of the cation buildup after over 2 h following removal of the external bias is somewhat surprising. A delayed SIMS measurement using a pixel charged 12 h prior (labeled '12 V delay') shows a near intrinsic profile, indicating that the junction is indeed dynamic, but that the redistribution of ions occurs very slowly after bias removal. Further, measurements on devices that had been sequentially charged under forward followed by reverse bias were performed for Li triflate LECs (Figure 2b). Results indicate that the cations built up from the first charging step do not fully redistribute even under reverse bias, rather the cations build up at both electrodes while depleting from the center of the polymer layer.

In addition to the study of lithium triflate based dynamic junction devices, we studied cation profiles in ATOA-AS based fixed junction devices that were charged approximately 12 h prior to performing SIMS. PIL LECs behave similarly to Li triflate LECs during forward bias charging, with a systematic cation buildup (indicated by detection of the CN^- ion) at the Au cathode with increased charging voltage, and visible depletion of cations at the ITO anode (Figure 3a). However, unlike for the Li triflate devices, the cation profile in PIL devices persists over 12 h after bias removal as well as after application of a reverse bias (Figure 3b). No noticeable buildup of cations at the ITO following application of reverse bias indicates that within the sensitivity of this measurement, the initial charging fully immobilized all cations in the device.

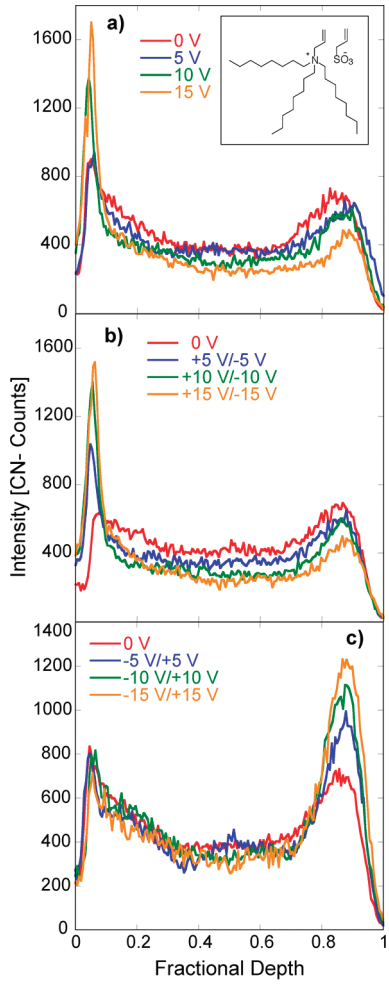

Figure 3. Relative intensities of the CN^- ion, a marker for the PIL cation, as a function of fractional depth into the polymer layer of PIL LECs as a function of charging voltage, (a) for devices charged using a forward bias, (b) for devices charged first under forward bias followed by charging under reverse bias, and (c) for devices charged under reverse bias. Scans taken approximately 12 h after charging. Inset shows the molecular structure of ATOA-AS.

These results confirm that the fixation of the junction occurs together with immobilization of the ions as previously suggested in the literature.[27] Reverse bias experiments confirm that cation buildup is always at the cathode and fixation occurs regardless of poling direction (Figure 3c). These results also show that the ion profiles established depend on the charging voltage even in the case of fixed junction devices, and suggest that fine-tuning of device performance may potentially be achieved through adjustments to charging procedure.

The results obtained here are particularly interesting in light of SKPM measurements reported by Pingree et al. and Rodovsky et al.[30,32] Results from those studies indicated that the voltage drop during charging in Li triflate LECs at the cathode reverts to the intrinsic state within one minute after the bias is removed. However, our results indicate that ion profiles even in lithium triflate devices take hours to relax to the intrinsic state. While these studies were performed with slightly different materials and device geometries, comparison of these results suggest that the observed rapid relaxation of the electric potential profile may not be correlated primarily to the migration/relaxation of the cations following bias removal. It

dx.doi.org/10.1021/am201469t | ACS Appl. Mater. Interfaces 2012, 4, 1149–1153

is possible, as some studies have suggested,[43,44] that highly localized n-doping does in fact occur in these devices, and that the observed relaxation of the electric potential profile correlates more directly to the reversal of this doping profile rather than to the redistribution of cations. For the IPM based devices explored in the study discussed above, both the electric potential and doping profiles are observed to remain fixed over much longer time scales.

In conclusion, using ToF-SIMS, we have measured directly the transient counterion profiles for cations in both Li triflate and PIL-based LECs. Our results are in good agreement with previous LEC studies, confirming the dynamic nature of Li triflate and the immobilization of counterion profiles for chemically fixed junction devices. For Li triflate LECs, results indicate a much slower redistribution of ions than previously assumed. For PIL LECs, the presence of a fixed junction is confirmed by the immobilization of the ion after initial poling even following application of a reverse bias. This technique may be used as a complementary characterization technique for understanding the depth profiles of ions in LECs and other devices for which the ionic carriers play a critical role.

EXPERIMENTAL SECTION

For Li triflate LECs, the salt was mixed with trimethylolpropane ethoxylate (TMPE) and Merck livilux polymer at a mass ratio of 0.025:0.075:1, respectively. Solvent used was 10 wt % cyclohexanone in chlorobenzene; the final solution being 1 wt % polymer mixture in solvent. TMPE and Li triflate were supplied by Aldrich and used as received. For PIL LECs, ATOA-AS and ADS 108GE polymer (American Dye Source, Inc.) were mixed at a mass ratio of 0.375:1 respectively. The mixture was dissolved at 4.5 wt % in chlorobenzene. The ATOA-AS was prepared as previously described.[10] Films were made by spin-casting the polymer solutions onto ITO coated substrates at 4000 rpm to a thickness of 100−200 nm, and then annealed under nitrogen for 1 h at ∼80 °C. The films were then dried under vacuum at 1×10^{-6} Torr overnight in a thermal evaporator before 40 nm thick Au electrodes were deposited. After a brief period in ambient conditions (<10 min), devices were transferred to a nitrogen atmosphere glovebox. Devices were constructed at Western Washington University (WWU) and then transported under inert conditions to the Environmental Molecular Science Laboratory (EMSL) at Pacific Northwest National Laboratory (PNNL). Both device charging (under inert atmosphere) and SIMS measurements were carried out at EMSL using a variety of procedures as described above. ToF-SIMS measurements were carried out at EMSL using a TOF.SIMS 5 spectrometer (IONTOF GmbH, Germany). A dual beam depth profiling strategy was performed. A 1.0 keV O_2^+ sputtering beam was used for positive ion depth profiling, and a 1.0 keV Cs^+ sputtering beam was used for negative ion depth profiling. The sputtering beams were scanned over a 300 μm × 300 μm area. A 25 keV Bi^+ analysis beam was used for data collection, and it was scanned over a 100 μm × 100 μm area at the center of the sputter crater.

AUTHOR INFORMATION

Corresponding Author

*E-mail: janelle.leger@wwu.edu.

Notes

The authors declare no competing financial interest.

ACKNOWLEDGMENTS

The authors gratefully acknowledge the Research Corporation Cottrell College Science Award, the National Science Foundation (CHE-0935920 and DMR-1057209), and Western Washington University for supporting this research. A portion of the research was performed using EMSL, a national scientific user facility sponsored by the Department of Energy's Office of Biological and Environmental Research and located at Pacific Northwest National Laboratory. The authors thank Drs. Laxmikant Saraf, Bruce Arey and the staff of EMSL for their assistance.

REFERENCES

(1) Forrest, S. R.; Thompson, M. E. *Chem. Rev.* **2007**, *107*, 925−927.
(2) Facchetti, A. *Chem. Mater.* **2011**, *23*, 733−758.
(3) MacDiarmid, A. G. *Angew. Chem., Int. Ed.* **2001**, *40* (14), 2581−2590.
(4) Leger, J. M. *Adv. Mater.* **2008**, *20*, 837−841.
(5) *Iontronics: Ionic Carriers in Organic Electronic Materials and Devices*; Leger, J. M., Berggren, M., Carter, S. A., Eds.; CRC Press: Boca Raton, FL.
(6) Pei, Q.; Yu, G.; Zhang, C.; Yang, Y.; Heeger, A. J. *Science* **1995**, *269*, 1086.
(7) van Reenen, S.; Matyba, P.; Dzwilewski, A.; Janssen, R. A.; Edman, L.; Kemerink, M. *J. Am. Chem. Soc.* **2010**, *132*, 13776−13781.
(8) Inganäs, O. *Chem. Soc. Rev.* **2010**, *39*, 2633−2642.
(9) DeMello, J. C.; Tessler, N.; Graham, S. C.; Friend, R. H. *Phys. Rev. B* **1998**, *57*, 12951−12963.
(10) Wagberg, T.; Hania, P. R.; Robinson, N. D.; Shin, J. H.; Matyba, P.; Edman, L. *Adv. Mater.* **2008**, *20*, 1744−1749.
(11) Kervella, Y.; Armand, M.; Stephan, O. *J. Electrochem. Soc.* **2001**, *11*, H155.
(12) Hu, Y.; Gao, J. *App. Phys. Lett.* **2006**, *89*, 253514.
(13) Edman, L.; Moses, D.; Heeger, A. J. *Synth. Met.* **2003**, *138*, 441−446.
(14) Habrard, F.; Ouisse, T.; Stephan, O.; Armand, M.; Stark, M.; Huant, S.; Dubard, E.; Chevrier, J. *Appl. Phys. Lett.* **2004**, *96*, 7219.
(15) Pachler, P.; Wenzyl, F. P.; Scherf, U.; Leising, G. *J. Phys. Chem. B* **2005**, *109*, 6020−6024.
(16) Shin, J. H.; Xiao, S.; Edman, L. *Adv. Funct. Mater.* **2006**, *16*, 949−956.
(17) Shin, J. H.; Matyba, P.; Robinson, N. D.; Edman, L. *Electrochim. Act.* **2007**, *52*, 6456−6462.
(18) Ouisse, T.; Stephan, O.; Armand, M. *Eur. Phys. J. Appl. Phys.* **2003**, *24*, 195−200.
(19) Anikeeva, P. O.; Madigan, C. F.; Halpert, J. E.; Bawendi, M. G.; Bulović, V. *Phys. Rev. B* **2008**, *78*, 085434.
(20) Coe-Sullivan, S.; Woo, W. K.; Steckel, J. S.; Bawendi, M.; Bulovic, V. *Org. Electron.* **2003**, *4*, 123−130.
(21) Leger, J. M.; Carter, S. A. *J. Appl. Phys.* **2005**, *98*, 124907.
(22) Gao, J.; Yu, G.; Heeger, A. J. *Adv. Mater.* **1998**, *10*, 692.
(23) Yu, G.; Cao, Y.; Andersson, M.; Gao, J.; Heeger, A. J. *Adv. Mater.* **1998**, *10*, 385.
(24) Chang, C. H. W.; Lonergan, M. C. *J. Am. Chem. Soc.* **2004**, *126*, 10536.
(25) Leger, J. M.; Patel, D. G.; Rodovsky, D. B.; Bartholomew, G. P. *Adv. Funct. Mat.* **2008**, *18*, 1212−1219.
(26) Li, Y.; Cao, Y.; Gao, J.; Wang, D.; Yu, G.; Heeger, A. J. *Synth. Met.* **1999**, *99*, 243−248.
(27) Kosilkin, I. V.; Martens, M. S.; Murphy, M. P.; Leger, J. M. *Chem. Mater.* **2010**, *22*, 4838.
(28) Leger, J. M.; Rodovsky, D. B.; Bartholomew, G. P. *Adv. Mater.* **2006**, *18*, 3130−3134.
(29) Tang, S.; Irgum, K.; Edman, L. *Org. Electron.* **2010**, *11*, 1079−1087.
(30) Pingree, L. S. C.; Rodovsky, D. B.; Coffey, D. C.; Bartholomew, G. P.; Ginger, D. S. *J. Am. Chem. Soc.* **2007**, *129*, 15903−15910.

(31) Bernards, D. A.; Flores-Torres, S.; Abruna, H. D.; Malliaras, G. G. *Science* **2006**, *313*, 1416.
(32) Rodovsky, D. B.; Reid, O. G.; Pingree, L. S. C.; Ginger, D. S. *ACS Nano* **2010**, *4*, 2673−2680.
(33) Lee, J. K.; Yoo, D. S.; Handy, E. S.; Rubner, M. F. *Appl. Phys. Lett.* **1996**, *69*, 1686.
(34) Handy, E. S.; Pal, A. J.; Rubner, M. F. *J. Am. Chem. Soc.* **1999**, *121*, 3525.
(35) Slinker, J. D.; Rivnay, J.; Moskowitz, J. S.; Parker, J. B.; Bernhard, S.; Abrun∼a, H. D.; Malliaras, G. G. *J. Mater. Chem.* **2007**, *17*, 2976.
(36) Slinker, J.; Bernards, D.; Houston, P. L.; Abruña, H. D.; Bernhard, S.; Malliaras, G. G. *Chem. Commun.* **2003**, 2392.
(37) Bolink, H. J.; Coronado, E.; Costa, R. D.; Orti, E.; Sessolo, M.; Graber, S.; Doyle, K.; Neuburger, M.; Housecroft, C. E.; Constable, E. C. *Adv. Mater.* **2008**, *20*, 1−4.
(38) Costa, R. D.; Pertegas, A.; Orti, E.; Bolink, H. J. *Chem. Commun.* **2010**, *22*, 1288−1290.
(39) Hoven, C. V.; Garcia, A.; Bazan, G. C.; Nguyen, T. Q. *Adv. Mater.* **2008**, *20*, 3793.
(40) Mouhib, T.; Delcorte, A.; Poleunis, C.; Bertrand, P. *Surf. Interface Anal.* **2011**, *43*, 175−178.
(41) Norrman, K.; Madsen, M. V.; Gevorgyan, S. A.; Krebs, F. C. *J. Am. Chem. Soc.* **2010**, *132*, 16883−16892.
(42) Steuerman, D. W.; Garcia, A.; Dante, M.; Yang, R.; Lofvander, J. P.; Nguyen, T. Q. *Adv. Mater.* **2008**, *20*, 528.
(43) Gao, J.; Dane. *J. Appl. Phys. Lett.* **2004**, *20*, 2778.
(44) Gao, J.; Dane. *J. Appl. Phys. Lett.* **2005**, *98*, 63513.